IMAGE-FORMING DETECTORS TO OBSERVE FINE SPATIAL DISTRIBUTIONS OF AURORAL X-RAYS

Yo Hirasima, Hiroyuki Murakami, Kiyoaki Okudaira,

Department of Physics, Rikkyo University, 34–1, Nishi-Ikebukuro 3-chome,
Toshima-ku, Tokyo 171

Masami Fujii, Jun Nishimura, Takamasa Yamagami

The Institute of Space and Astronautical Science, 6–1, Komaba 4-chome,
Meguro-ku, Tokyo 153

and

Masahiro Kodama

Yamanashi Medical College, Tamaho-mura, Nakakoma-gun, Yamanashi 409–38

Abstract: Observations of fine auroral X-ray images at balloon altitude are important for studies of acceleration and precipitation mechanisms of energetic particles in the magnetosphere. Balloon-borne auroral X-ray image-forming detectors with some angular resolution are proposed to observe spatial distributions of auroral X-ray sources, as fine as possible and also as a function of time.

Two systems of image-forming detectors are being developed. One system consists of two sets of NaI(Tl) scintillation detectors with very thin scintillators. The first set has a collimator with multi-pinholes, giving an angular resolution of 5°. The second has a collimator with a single larger pinhole, and it eliminates the redundant images unavoidable in the multi-pinhole type of detector. The incident position of an X-ray on the thin scintillator is determined by using the signals from four photomultiplier tubes attached to the scintillator.

The other system is constructed with the NaI(Tl) scintillator viewed by a micro-channel plate photomultiplier tube (MCP PMT) through a Fresnel lens. The pinhole aperture of the collimator is selected according to the auroral X-ray intensity, giving an angular resolution of 2°, 5° or 10°. It is expected that auroral X-ray images can be observed with an angular resolution of 5° and with a time resolution of 1 s, for the moderate activity of an auroral X-ray burst.

1. Introduction

For many years, the development of an image-forming detector has been in progress to observe spatial distributions of auroral X-rays. The intensity of auroral X-rays is quite high, compared with those of Galactic X-rays and the sources are spread widely in the whole sky. Also, the source intensity of auroral X-rays changes rapidly with time. In the case of the auroral X-ray microburst, time variations in intensity are as short as 0.1 s. Thus, an image-forming detector is necessary which can measure the change of spatial distributions of auroral X-ray sources with better resolution of

169

time.   The present authors now have, under development, new types of image-forming detectors to observe the fine auroral X-ray spatial distributions with a short period.

At present, as for the generation mechanism of the substorm in the magnetosphere, many workers are essentially in agreement with the model of the day-side substorm (PERREAULT and AKASOFU, 1978; AKASOFU and KAMIDE, 1980).   On the other hand, the model for the night-side substorm mechanism has not been agreed on so far.   There are two main views of substorm models related with the magnetotail (AKASOFU, 1978; NISHIDA, 1978).   One is that the reconnection of magnetic field lines happens to occur in 15–20 R_E (R_E: the earth radius) of the magnetotail, and the energetic particles are accelerated there.   The other is the electric current disruption model.   According to this model, when the cross-tail currents in 15–20 R_E of the magnetotail decrease, the field-aligned currents along the magnetic field lines increase so that the dynamo system is constructed through the magnetotail currents, the field-aligned currents, and the ionospheric electrojet currents in the polar region.   Hence, the precipitating auroral particles are accelerated in the field-aligned electric fields.   The acceleration of low energy particles could be possible, adopting either of the two above-mentioned models. However, it seems that the X-line model is favorable for the acceleration of the electrons with more energies than several tens of keV (TERASAWA and NISHIDA, 1976).   In order to confirm this picture, experimental investigations of high energy particle phenomena are desirable and valid.   The energetic precipitating electrons produce auroral X-rays through the bremsstrahlung in the atmosphere at about 100 km altitude.   As the auroral X-rays with several tens of keV are produced by the primary precipitating electrons with higher energies, the auroral X-rays with high energies would reflect directly the state of high energy particle acceleration in the X-line region deep in the magnetosphere, and also, populations of energetic electrons at the equatorial geosynchronous orbit vary rapidly in substorms (*e. g.*, MCILWAIN, 1975; WALKER *et al.*, 1975; PARKS *et al.*, 1977).   This fact might be connected with spatial structures of auroral X-ray sources, including temporal variations, because convection exists in the magnetosphere.   Observations of fine auroral X-ray images in which geomagnetical directions are defined can hardly ever be obtained.   Thus, fine distributions of auroral X-ray sources in the auroral zone and time variations of these distributions are not so clear at present. Comparison among visible, UV and X-ray images of aurora would reveal origins of the different components, *i. e.*, low energy electrons and high energy electrons.   Also, a possible difference in the auroral X-ray spatial distributions between the dawn side and the dusk side is to be examined.

In general, there are two ways of observing auroral X-ray spatial distributions. One is to use a space-vehicle such as a balloon, a rocket or a satellite.   The other is to make simultaneous balloon observations in two or more auroral zone sites.

Observations of auroral X-ray spatial distributions by using a single space-vehicle were performed by PARKS (1967), KODAMA and OGUTI (1976), and YAMAGAMI *et al.* (1978).   In most of these observations, the sky was scanned by X-ray telescopes with a resolution angle of $\geq 20°$, and thus the observations of the spatial distributions were limited to a certain degree due to rapid time variations in auroral X-ray sources.

Recently, MAUK *et al.* (1981) observed auroral X-ray images with a resolution angle of 13° (equivalent to 15 km at 100 km height), using a balloon-borne image-

froming detector, a type of pinhole camera, by which short term variation in spatial distribution was observed. IMHOF *et al.* (1980) observed the world-wide distributions of auroral X-ray sources using CdTe semiconductor detectors on board a satellite. Satellite observations are suitable to detect world-wide characteristics of phenomena, but the rapid movement and the spinning motions of the satellite prevent observing fine spatial structure of auroral sources. Thus, the spatial resolution observed by IMHOF *et al.* (1980) was limited by 130 km even for the case of a time resolution of 0.5 s.

In all of the simultaneous observations of auroral X-rays by means of many balloons (BJORDAL *et al.*, 1971; KREMSER *et al.*, 1973; MARAL *et al.*, 1973; ULLALAND, 1979; ZHULIN and LAZUTIN, 1979), simple X-ray detectors consisting of G-M tubes or single scintillation counters were used. Accordingly, although studies on the large-scale dynamics of particle precipitation over the auroral oval were possible, studies on its fine-scale dynamics were not feasible in this case.

Thus, it is quite desirable to prepare a detector with a fine space resolution, say 5°, and with a moderate time resolution. If the auroral X-ray images observed by a balloon-borne image detector with an angular resolution of 5°, a spatial resolution of 6 km can be obtained in the auroral X-ray source layer. This spatial resolution makes it possible to reveal relation between energetic precipitating particles and auroral break-up events. In the present paper, two types of image-forming detectors are proposed to meet this requirement.

2. Multi-Pinhole Camera Type of Image-Forming Detector

First, the auroral X-ray image-forming detector consisting of a thin NaI(Tl) scintillator and a pinhole collimator will be described. The detector was designed for observations by balloon. It is a modification of the detector used by MAUK *et al.* (1981). By a combination of the detector with a single pinhole collimator of wide field of view and a detector with a multi-pinhole collimator of fine field of view, a complete image detector set is constructed. As shown in Fig. 1a, a fine structure of auroral X-ray image can be observed by the detector with a collimator having several small pinholes. Since the number of pinholes is plural, images are redundant. To eliminate this redundancy, another detector with a single pinhole is used, giving coarse spatial resolution, as shown in Fig. 1b. Also, the latter detector with wide field of view is useful to observed an auroral X-ray burst of small activity, although spatial resolution is coarse. Therefore, the dynamic range can be extended to make it possible to detect auroral X-ray burst activities of various amounts. An important feature of this combined set of detectors is that it has a large aperture which keeps the angular resolution of the image detector finer than the detector used by MAUK *et al.* (1981). The multi-pinhole camera type of the image-forming detector is very useful to observe rapid time variation and spatial movement of a discrete auroral X-ray source with a fine spatial resolution.

A preliminary design for the detector is shown in Fig. 1. The thin NaI (Tl) scintillator is used to detect the positions where X-rays are absorbed in the scintillator. The technique to determine the positions where X-rays are absorbed is the same as that used by MAUK *et al.* (1981). It is assumed that the individual positions are identified for
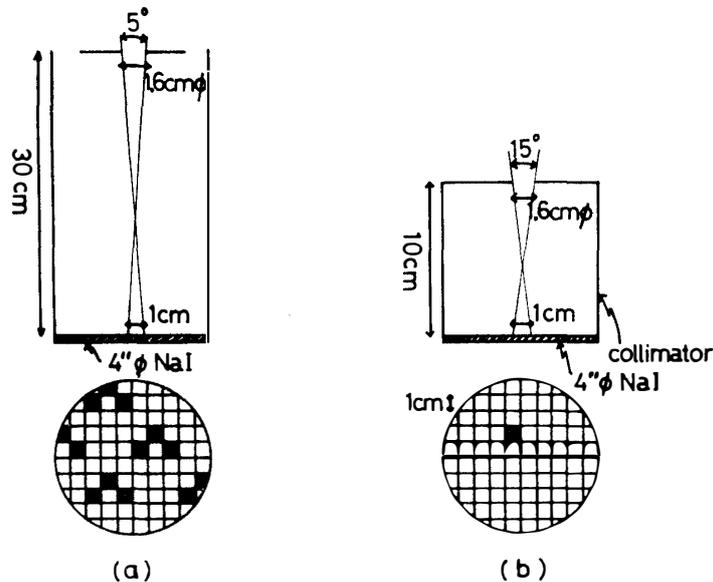
Fig. 1. Multi-pinhole camera type of auroral X-ray image-forming detector. (a) detector
with collimator having several small pinholes. (b) detector with collimator having
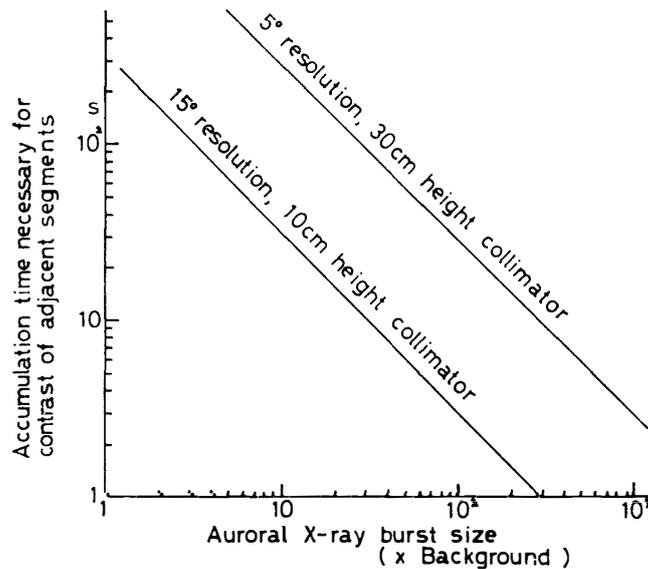a single large pinhole.

Fig. 2. Relation between the activity size of the auroral X-ray burst and the data accumulation
time, used to discriminate two adjacent segments from each other.

each of the 1 × 1 cm segment units.   When the intensity of the X-rays is high enough,
the accumulation time necessary to construct the image of the auroral X-rays is short.
Relationship between the activity of the auroral X-ray burst and the accumulation time
necessary to construct the spatial structure of the image was estimated.   The results are
shown in Fig. 2.   When a ratio of auroral X-ray counts in two adjacent segments in
the scintillator was 2 : 1, the accumulation times necessary to give contrast beyond the
statistical fluctuation are shown as the function of the auroral X-ray burst sizes.   A cri-
terion that $S/\sqrt{N}$ ratio is 2, is adopted (S: a signal count; N: a background count).

The signal count depends on the auroral X-ray burst size. The size of the burst is expressed as the multiple in terms of background count. For active auroral X-ray bursts, intensity enhancements of 10^2 times the background or greater are sometimes observed. In this case, an intensity of auroral X-rays of 15–85 keV amounts to 3×10^2 photon/(cm$^2 \cdot$s$\cdot$sr) or greater. For example, if the intensity increase is 3×10^2 or 3×10^3 times the background, angular resolution of image of 15° or 5° is obtained in a time resolution of 1 s with the $S/\sqrt{N}$ ratio of 2. Detection limits of auroral X-ray images are inferred from Fig. 2, depending on auroral X-ray burst sizes. If the count ratio between two adjacent segments is larger than 2, the accumulation time necessary to get good contrast of image is shorter than those shown in Fig. 2.

On visual auroras, structures and break-up phenomena of aurora arcs are known well at present. However, in X-ray energy range, fine spatial structures of auroral X-ray illuminating regions are not known so well for the present. Although fold structures in the auroral X-ray illuminating regions were observed with time resolution of about 5~10 s (KODAMA and OGUTI, 1976; MAUK et al., 1981), descrete arc structure as curtain-like one is not defined in the X-ray energy range. If auroral X-ray images are observed with spatial resolution of several km and time resolution of order of 1 s, it will be clear whether descrete arc structure in auroral X-ray illuminating region is present or not. In structures and dynamics of auroras, comparison between visual auroras and auroral X-ray sources is interesting.
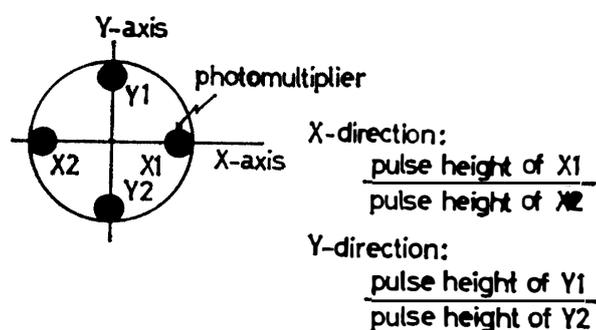

Fig. 3. Method to obtain auroral X-ray images using four photomultiplier tubes. One detector has a collimator with multi-pinholes. The other detector has a collimator with a single larger pinhole.

To identify the position where an X-ray has hit, four photomultiplier tubes are used as shown in Fig. 3. This method has already been established by MAUK et al. (1981). Two photomultiplier tubes are put in the two ends of the X-axis direction and the other two tubes are put in the two ends of the Y-axis direction. The ratio of both pulse heights from the photomultiplier tubes $X1$ and $X2$ is used to determine the incidence position of the X-ray on the X-axis direction, i. e., the X-coordinate, and a similar ratio between the photomultiplier tubes $Y1$ and $Y2$ is used to determine the Y-coordinate. The X-ray incidence positions are determined by the X- and Y-coordinate diagram, and then the auroral X-ray images are built up.

3. Auroral X-Ray Image-Forming Detector Using a Microchannel Plate Photomultiplier Tube (MCP PMT)

Differing from the method described in the preceding paragraph, another method using the microchannel plate photomultiplier tube (denoted by MCP PMT, hereafter) will be proposed next. Recently, the development of MCP PMT has been remarkable (*e. g.*, many articles appeared in IEEE Trans. Nucl. Sci., February 1981.); and a spatial resolving power of $\sim 1/10$ mm is available with these MCP PMT. Quantum efficiency of photocathode and an electron gain in MCP PMT have been developed to be almost the same as an ordinary photomultiplier tube. Thus, it has become possible to apply MCP PMT to detecting the image of auroral X-rays.

In this case, a NaI(Tl) scintillator with a single-pinhole collimator was used. As shown in Fig. 4, photons from the thin NaI(Tl) scintillator were focussed through a Fresnel lens into the image on the photocathode of MCP PMT. A Fresnel lens with a small F number was necessary to collect the scintillation light effectively. A $3''$ ϕ NaI(Tl) scintillator with 3-mm thickness was used. The $3''$ ϕ image on the NaI (Tl) scintillator was converted into an $1''$ ϕ image on the photocathode of MCP PMT. If the positional resolution on the photocathode was 1 mm, with a margin, the corresponding positional resolution on the scintillator was 3 mm. Hence, the spatial resolution of the auroral X-ray image depended mainly on the pinhole aperture. Therefore, the detector is constructed so that the aperture can be changed by a rotating shutter with different diameters of pinholes, as shown in Fig. 4. Depending on the intensity of the auroral X-rays, the appropriate diameter of pinhole can be selected. In this design, the angular resolution of the detector is fixed at $2°$, $5°$ or $10°$.
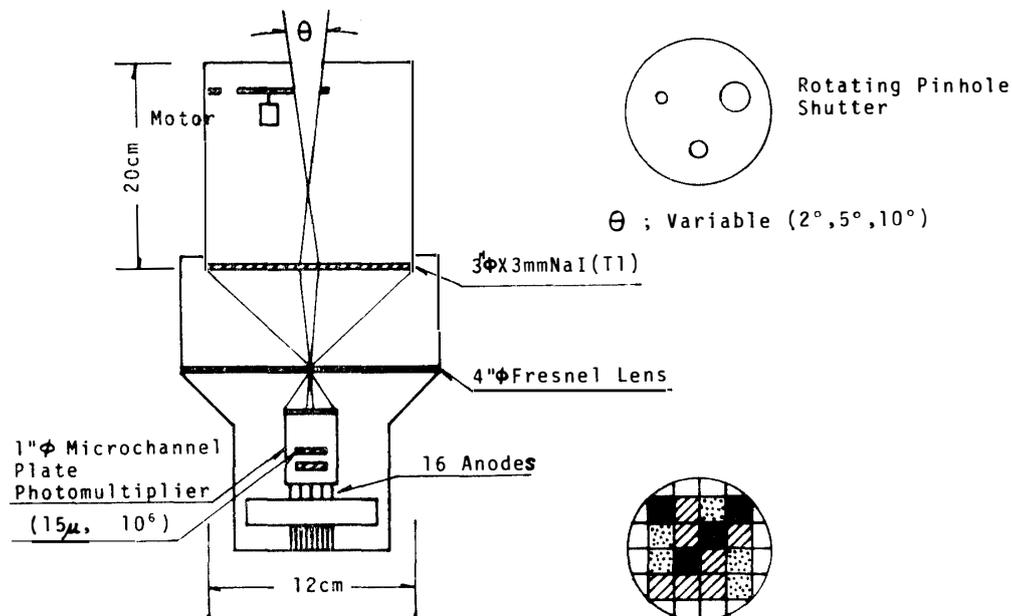

Fig. 4. Auroral X-ray image-forming detector using a microchannel plate photomultiplier tube (*MCP PMT*). The sensitive area of NaI(Tl) is subdivided into 1-cm×1-cm segments. These segments correspond to images of 0.33×0.33 cm in size on the photocathode of MCP PMT. The aperture of the single pinhole can be changed to correspond with the auroral X-ray intensities, giving an angular resolution of 2°, 5° or 10°.
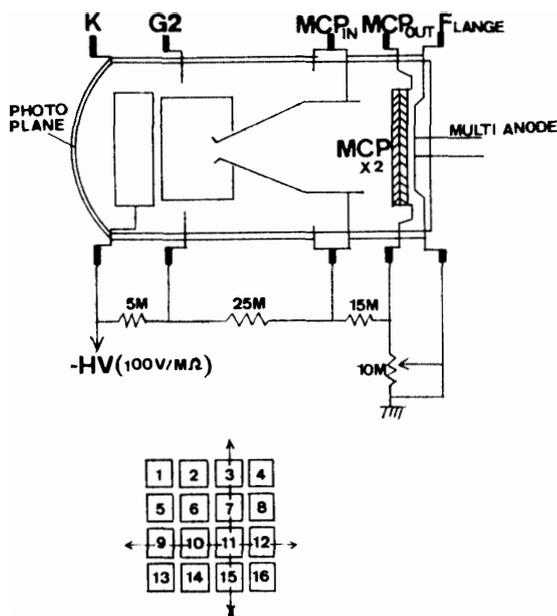
Fig. 5.   Structure of the microchannel plate photomultiplier tube (MCP PMT), Hamamatsu TV
         R1224, with 16 anodes.

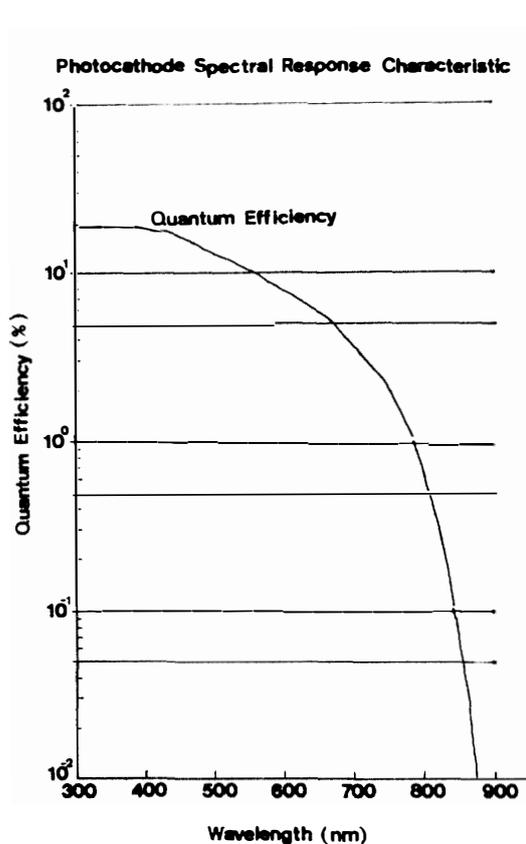Fig. 6.   Spectral response characteristics of
         the photocathode of the microchannel
         plate photomultiplier tube (MCP
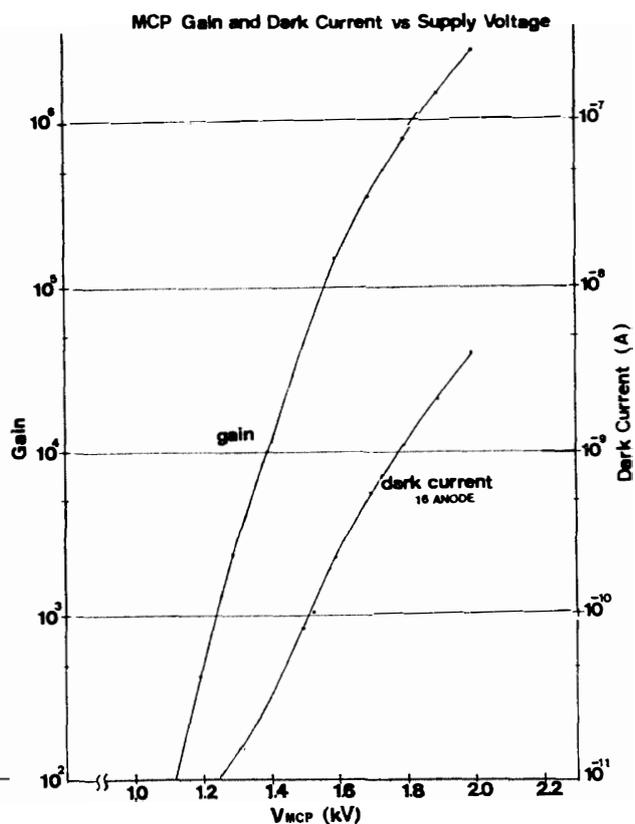   PMT) R1224.

Fig. 7.   Microchannel plate (MCP) gain and
         dark current as a function of voltage
         supply, for R1224.

The structure of MCP PMT, R1224, used here, is shown in Fig. 5. The photocathode is an 1″ ϕ multi-alkali type. The quantum efficiency of the photocathode is shown in Fig. 6. This type of MCP PMT has 16 anodes. The microchannel plate (MCP) is of V-shape type with two stages. An electron gain by MCP and its dark currents are shown in Fig. 7. The wavelength in which the maximum fluorescence intensity of NaI (Tl) is detected is 410 nm, and the wavelength width is about 100 nm at FWHM. The quantum efficiency is about 20% in this wavelength range. The electron gain by MCP is 2×10^6, when a high voltage of 2 kV is supplied. This electron gain is the same as that of a standard type of photomultiplier tube. The dark currents which have the principal effect on the S/N ratio are lower than those of the standard type of photomultiplier tube. Now, we estimate the number of photons which arrive at the photocathode of MCP PMT. The radius and the focal length of the Fresnel lens are denoted by R and f. The index of light-collecting ability of the lens is an F number. The distance between NaI(Tl) and the Fresnel lens is denoted by l. When an image of the 3″ ϕ NaI(Tl) is focussed on the 1″ ϕ photocathode of MCP PMT, $l=4f$ holds. Also, at NaI(Tl) position, the aperture's solid angle Ω subtended by the Fresnel lens is approximately expressed by

$$\Omega \simeq \frac{\pi R^2}{l^2} = \frac{\pi R^2}{(4f)^2} = \frac{\pi}{64} \cdot \frac{1}{F^2} .$$

The fraction of light thrown from NaI(Tl) to the Fresnel lens is, therefore,

$$\frac{\Omega}{2\pi} = \frac{1}{128} \cdot \frac{1}{F^2} .$$

A Fresnel lens having an F number of 0.6 and a transparency of about 80% is available. With such a lens, a fraction of about 1/60 of the light emitted from NaI(Tl) can arrive at the photocathode of MCP PMT. A single incident X-ray with 30 keV is expected to produce about 700 photons in NaI(Tl). About 300 of these are expected to go outside NaI(Tl), because of the difference of refractive indexes between NaI(Tl) and air. Accordingly, about 5 photons are expected to arrive at the photocathode, and it looks to be possible to detect X-rays with an energy of 30 keV. However, detections of low energy X-rays with ≲30 keV are marginal in this detector system, because the number of photons expected to arrive at the photocathode is small and fluctuates. In oder to detect surely these low energy X-rays, it may be necessary to connect the photocathode of MCP PMT with the NaI(Tl) scintillator optically through a bundle of thin light guides providing desirable spatial resolution. Energetic X-rays with about 100 keV, which are observed in a substorm, are easier to be detected.

Variation in anode currents of MCP PMT is shown in Fig. 8, when the illuminated position on the photocathode of MCP PMT moves. The measurement was made by moving the position of weak spot-beam light from LED, of which the diameter was 1 mm. Favorable size of one segment unit in NaI(Tl) was 1 cm in length, which corresponds to 3.3 mm on the photocathode of MCP PMT. Such position resolution is possible by measuring anode currents and by comparing difference in currents of adjacent anodes. The current ratio between adjacent anodes is an indication of the illuminated position on the photocathode. Differences in the peak current values among

Fig. 8. *Variation in anode currents of the micro-channel plate photomultiplier tube (MCP PMT), when illuminated position on the photocathode moves. Numbers attached to curves represent order-numbers of anodes; 1 mm on the photocathode corresponds to 1 section of abscissa of the graph.*
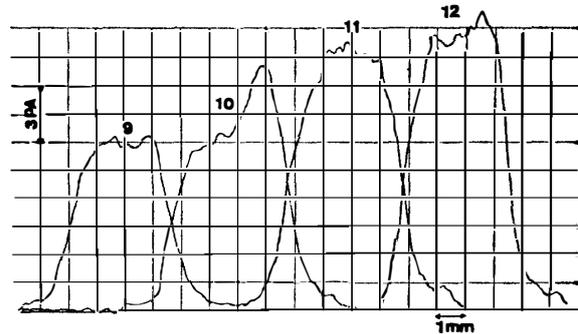
the anodes are compensated for by adjusting the amplifier gain. A block diagram of balloon-borne electronic circuits is shown in Fig. 9.

The Fresnel lens to be used should have a small *F* number of 0.6, which means a fairly good ability of light-collecting. Qualities of an image viewed through this Fresnel lens were tested. In Fig. 10, the pattern used in the test and its image are shown.
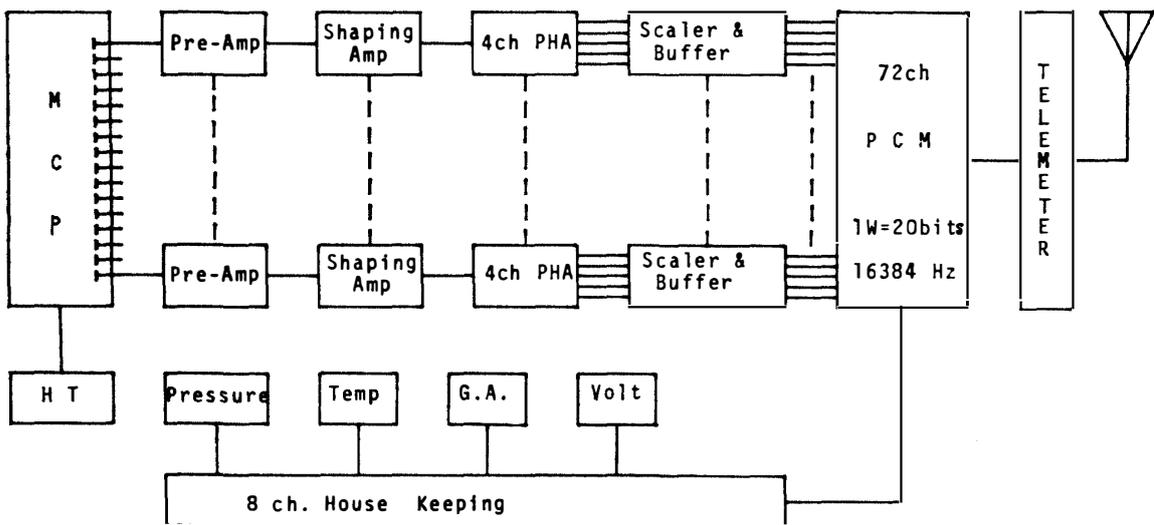

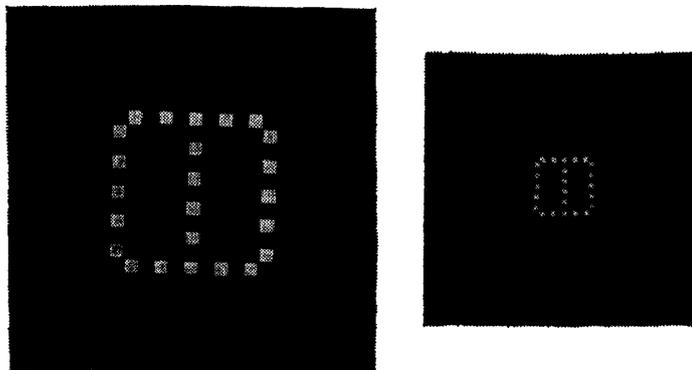Fig. 9. *Block diagram of balloon-borne electronic circuits.*

Fig. 10. *Pattern used in image-forming test of the Fresnel lens (left) and the image viewed through a lens with an F number of 0.6 (right). The pattern is formed by arrangement of 0.5 × 0.5 cm square holes.*

The size of a square hole in the pattern is 0.5×0.5 cm.   Judging from the clearness of the image of the pattern, a spatial resolution of 0.2 cm is achieved on the original pattern.   Therefore, the spatial resolution of a 1-cm×1-cm segment in NaI (Tl) can be maintained.

If MCP PMT with more multi-anodes or a resistive type of anode is used, it is possible to obtain better a spatial resolution of ∼1/10 mm on the photocathode, which is a characteristic of MCP PMT.   Thus, very fine auroral X-ray images can be obtained in spite of their rapid time variations.

Acknowledgments

References

AKASOFU, S.-I. (1978):   The interaction between a magnetized plasma flow and a magnetized celestial body: A review of magnetospheric studies.   Space Sci. Rev., **21**, 489–526.

AKASOFU, S.-I. and KAMIDE, Y. (1980):   Recent progress in studies of magnetospheric storms and substorms.   J. Geomagn. Geoelectr., **32**, 585–615.

BJORDAL, J., TREFALL, H., ULLALAND, S., BEWERSDORFF, A., KANGAS, J., TRANSKANEN, P., KREMSER, G., SEAGER, K. H. and SPECHT, H. (1971):   On the morphology of auroral-zone X-ray events —I.   Dynamics of midnight events.   J. Atmos. Terr. Phys., **33**, 605–626.

IMHOF, W. L., KILNER, J. R., NAKANO, G. H. and REAGAN, J. B. (1980):   Satellite X ray mappings of sporadic auroral zone electron precipitation events in the local dusk sector.   J. Geophys. Res., **85**, 3347–3359.

KODAMA, M. and OGUTI, T. (1976):   Spatial distributions of auroral zone X-rays as viewed from rocket altitudes.   Mem. Natl Inst. Polar Res., Ser. A (Aeronomy), **14**, 1–58.

KREMSER, G., WILHELM, K., RIEDLER, W., BRØNSTAD, K., TREFALL, H., ULLALAND, S. L., LEGRAND, J. P., KANGAS, J. and TANSKANEN, P. (1973):   On the morphology of auroral-zone X-ray events—II.   Events during the early morning hours.   J. Atmos. Terr. Phys., **35**, 713–733.

MARAL, G., BRØNSTAD, K., TREFALL, H., KREMSER, G., SPECHT, H., TANSKANEN, P., KANGAS, J., RIEDLER, W. and LEGRAND, J. P. (1973):   On the morphology of auroral-zone X-ray events — III.   Large-scale observation in the midnight-to-morning sector.   J. Atmos. Terr. Phys., **33**, 735–751.

MAUK, B. H., CHIN, J. and PARKS, G. (1981):   Auroral X-ray images.   J. Geophys. Res., **86**, 6827–6835.

MCILWAIN, C. E. (1975):   Auroral electron beams near the geomagnetic equator.   The Physics of the Hot Plasma in the Magnetosphere, ed. by B. HULTQUVIST and L. STENFERO.   New York, Plenum Press, 91.

NISHIDA, A. (1978):   Geomagnetic Diagnosis of the Magnetosphere.   New York, Springer.

PARKS, G. K. (1967):   Spatial characteristics of auroral-zone X-ray microbursts.   J. Geophys. Res., **72**, 215–226.

PARKS, G. K., LIN, C. S., MAUK, B., DEFOREST, S. and MCILWAIN, C. E. (1977):   Characteristics of magnetospheric particle injection deduced from events observed on August 18, 1974.   J. Geophys. Res., **82**, 5208–5214.

PERREAULT, P. and AKASOFU, S.-I. (1978):   A study of geomagnetic storms.   Geophys. J. R. Astron. Soc., **54**, 547–573.

TERASAWA, T. and NISHIDA, A. (1976):   Simultaneous observations of relativistic electron bursts and neutral-line signatures in the magnetotail.   Planet. Space Sci., **24**, 855–866.

ULLALAND, S. (1979):   SBARMO-78 auroral zone balloon programme during IMS.   Advances in

Space Exploration COSPAR Symposium Series, 5, Scientific Balloon. Oxford, Pergamon Press, 83 p.

WALKER, R. J., ERICKSON, K. N., SWANSON, R. L. and WINCKLER, J. R. (1975): ATS-6 synchronous orbit trapped radiation studies with an electron-proton spectrometer. IEEE Trans. Aerosp. Electron. Syst., 11, 1131–1137.

YAMAGAMI, T., FUJII, M., NISHIMURA, J., MURAKAMI, H., HIRASIMA, Y., KAJIWARA, M., OKUDAIRA, K. and KODAMA, M. (1978): Balloon observations of auroral X-rays in Canada. I. Determination of auroral X-ray illuminating regions. J. Geomagn. Geoelectr., 30, 663–682.

ZHULIN, I. A. and LAZUTIN, L. L. (1979): The project "synchronous auroral multiple balloon observatories (SAMBO)". Advances in Space Exploration COSPAR Symposium Series, 5, Scientific Balloon. Oxford, Pergamon Press, 89 p.